

Extrapolation Function Selection for the Prediction of High-Load Responses from Low-Load Biomechanical Data

V. C. Chancey, R. W. Nightingale, M. B. Nebel,
J. F. Luck, and B. S. Myers

ABSTRACT

Nondestructive low-load experiments are often used to determine stiffness properties of biological specimens. After regressing this low-load behavior to determine a representative property curve, extrapolation of the property curve is required to define behavior beyond the regressed region. The resulting model is assumed to represent behavior of the system to failure. However, an extrapolated function may incorrectly predict behavior outside the regressed range, and no data on the validity of the extrapolation are usually available. To study this problem for cervical spine specimens, three types of functions were evaluated: (1) nonlinear extrapolation of the best-fit exponential function, (2) linear extrapolation, and (3) nonlinear extrapolation of the best-fit polynomial function. Nonlinear stiffness curves from nondestructive testing in two modes of loading, pure tension and pure bending, were extrapolated to predict failure. These predictions were then compared to known failure responses and appropriate extrapolation functions were recommended.

INTRODUCTION

Experimental studies of biologic structural properties are often limited by specimen availability and specimen degradation in vitro. As such, an experimental study can only investigate a limited number of physiological and even more limited number of injurious responses. Nondestructive testing typically describes mechanical testing at low-load levels, within the elastic range, that determines structural properties. Destructive testing involves biomechanical failure and injury to quantify tolerance. Unfortunately, the high-load behavior located between the low-load behavior quantified with nondestructive testing and failure is rarely described. As a result, low-load structural property research frequently forms the basis for models that are expected to respond to physiological exposures, rarely injurious, and injurious levels of loading. Consequently, modelers often must guess at how best to represent the high load structural behavior. This study explores the use of some extrapolation functions for bridging the gap between low-level behavior

and failure data using nondestructive and destructive test data derived from cervical spine pure tension and pure bending tests.

METHODS

Two cervical spine studies, pure tension and pure bending (Nightingale et al., 2002), including experimental nondestructive low-load stiffness testing and failure testing, provided data for this study.

Tension Experimental Study

Specimen Preparation: Unembalmed male human cadaver specimens from the head through T1 were obtained. Eight specimens, 45 to 68 years old (average age 59 ± 8 yrs), were tested after their structural integrity was assured by physical examination and review of medical records and pretest radiographs of the specimens. To begin, the musculature and mandible were removed to better visualize the cervical spine motions and injury mechanisms. The removal of the mandible also allowed application of load to the maxilla. The skull was coupled to the head mount platform using bone screws and polymethylmethacrylate (PMMA), so that the head mount platform was parallel to the Frankfort plane. Care was taken to allow full motion at the Occiput-C1 level. In addition, the mount points of the skull were chosen remote from the base of the skull to mitigate any stress concentrations in the regions where basilar skull injuries commonly originate (McElhaney et al., 1995). T1 was cast into an aluminum cup with molded PMMA and reinforced polyester resin. The cast allowed free motion at the C7-T1 level and oriented the T1 vertebra 25° down from the horizontal (-25° pitch) to preserve normal cervical lordosis (Matsushita et al., 1994).

Test Protocol: The head and neck were placed in the experimental test frame (Van Ee et al., 2000) (Figure 1). The head mount platform was adjusted within the experimental frame to ensure the Frankfort plane horizontal for the reference position. The test fixture applied a pure vertical load (based on the global coordinate system) at the center of the rotational bearing aligned with an anatomical point-of-interest. Pure tensile loading was obtained by use of the linear and rotational bearings coupling the head carriage, containing the head mount platform, to the test frame. An RVDT located at a rotational bearing quantified head rotation. Two LVDTs were used to monitor the hydraulic actuator position and the linear bearing position. A six axis Denton load cell coupled the lower portion of the spine to the MTS hydraulic actuator. Data were collected using a digital data acquisition system (National Instruments; Austin, TX).

All testing was performed under load control. The initial position with Frankfort plane horizontal was re-established before each test with no load applied, resulting in a slightly pre-tensed specimen. After the nondestructive whole spine testing, the specimen was removed from the load frame and sectioned for motion segment testing. The spine was sectioned between C3-C4 and C5-C6 to give three intact motion segments for testing that included the adjacent vertebral bodies and intact ligamentous structures. The resulting segments, Occiput-C2 (n=4), C4-C5 (n=8), and C6-C7 (n=6), were then cast to produce motion segment test specimens. Each single vertebra was cast using supra-pedicular loops traveling from the casting material through the vertebral foramen over the pedicle and back through the transverse foramen. In addition, crossed k-wires were also used to couple the specimen to PMMA and bone screws with a fiber-reinforced resin. For the upper cervical segment, two vertebrae (C2, C3) were cast together using a combination of bone screws and k-wires pre-molded with PMMA into fiber-reinforced resin.

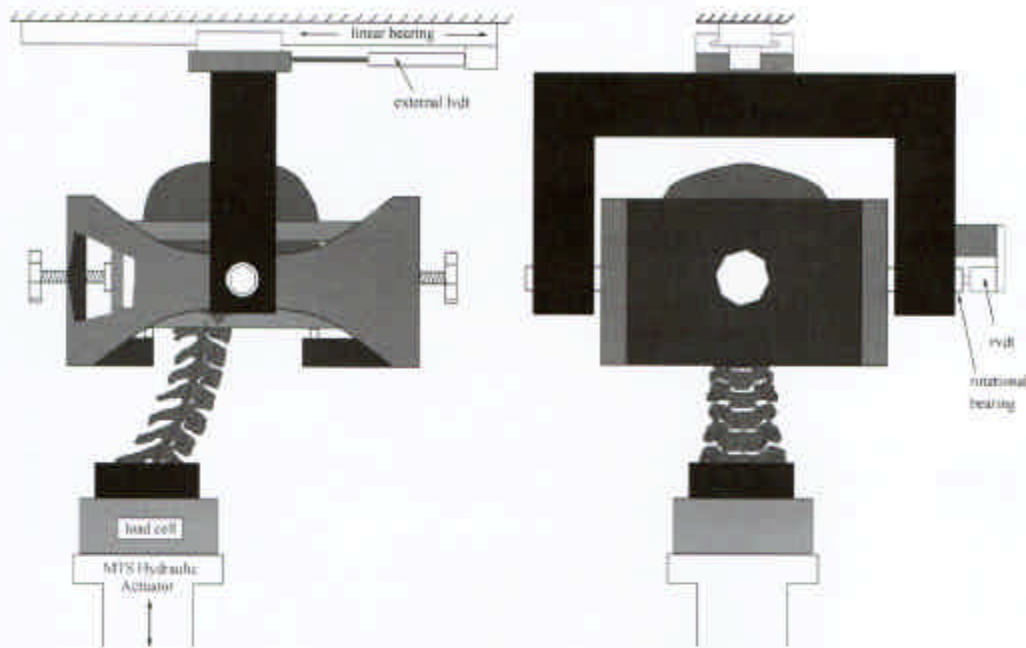


Figure 1. Test fixture for the tensile test experiments. The fixture produces a pure vertical load at the center of the rotational bearing through the use of linear and rotational bearing that minimized the shear and rotational moment respectively.

After pre-conditioning with 60 cycles of a 1 Hz sine wave with mean and amplitude of 75N of tension, a battery of nondestructive tests were performed on the whole cervical spine. The Occiput-C2 (O-C2) segment was likewise pre-conditioned and tested nondestructively. The nondestructive testing of O-C2 included a 300 N (50 N/s) stiffness test with the load line of action passing through the occipital condyles. Finally the O-C2 segment was failed at 1000 N/s with the load line of action through the occipital condyles. Rotation and linear anterior-posterior (A-P) translations were allowed for the 300 N stiffness test and the failure test. Loading through the occipital condyles for both the low-load stiffness test and failure resulted in negligible A-P translation (<1.5 mm) and rotation (<1.6 degrees) of the head. The lower motion segments, C4-C5 and C6-C7, were pre-conditioned and tested nondestructively. A 300 N (50 N/s) stiffness test with free cranial end conditions was performed before failure (1000 N/s) with identical cranial position and end conditions. All failure tests were imaged at 50 frames/second. Sub-catastrophic failures, including yielding (increasing specimen length, but constant load) and micro-failures (sharp decreases in load), prior to ultimate failure were identified. Specimen dissection was performed to document injuries.

Bending Experimental Study

Specimen Preparation: Unembalmed female human cadaveric cervical spines were tested. Paired stiffness and failure tests were performed on 35 spinal segments from 13 unembalmed cervical spines. Donor age ranged from 33 to 66 years (average age 50 ± 8 yrs). The muscular tissues were removed while keeping all the ligamentous structures intact (with the exception of the ligamentum nuchae). All specimen handling was performed in compliance with CDC guidelines (Cavanaugh and King, 1990). The cervical spines were sectioned into 4 groups: O-C2 (n=8), C3-C4 (n=8), C5-C6 (n=9), and C7-T1 (n=10). The lower cervical motion segments were cleaned and cast into aluminum cups with fiber-reinforced polyester resin. The cephalad end of the upper cervical spine specimens was secured using halo fixation. The mandible and maxilla were removed in order to

allow unimpeded range of motion. Upper cervical specimens (O-C2) were inverted and mounted in the test frame using halo fixation of the head and casting of the C2 vertebra.

Test Protocol: Bending tests were performed in a pure moment test frame. The moments were generated using a pair of free-floating precision pneumatic pistons to apply a force-couple. The resulting angular displacements were computed by tracking markers on digital images (Figure 2). After the specimen was mounted in the test frame, a counterweight was applied to the upper casting assembly. The mass of the counterweight counterbalances the mass of the assembly and applies 0.5 Newtons of tension on the vertebra, creating a repeatable initial position in the middle of the neutral zone. The specimen was imaged in the initial position and the load cell was zeroed. This image served as the initial reference image for all tests. After digitization of the centroid locations for markers in each image, angular displacements for each image were determined with respect to the reference image.

Prior to flexibility testing, the specimens were preconditioned with 30 cycles of ± 1.5 N-m of moment. To determine their flexibilities, each specimen was loaded with pure flexion and extension moments in 0.5 N-m increments. Thirty seconds of creep was allowed prior to data acquisition, and the load was released between load steps. The peak applied-moment was approximately 3.5 N-m. A six-axis GSE load cell at the base of the specimen was used to measure the applied moment and to ensure that the moment remained pure. The load application, test duration, data acquisition, and load release were all controlled by PC based software (National Instruments; Austin, TX).

For failure testing, the counterweight was removed and the specimens were failed in either flexion or extension. The loading rates were dependent on the flexibility of the specimen and were approximately 90 N-m/second. These tests were imaged at 125 frames/second. Failures were defined as a decrease in the measured moment with increasing rotation, and they were verified by examination of the high-speed images. Specimen dissection was performed to document injuries.

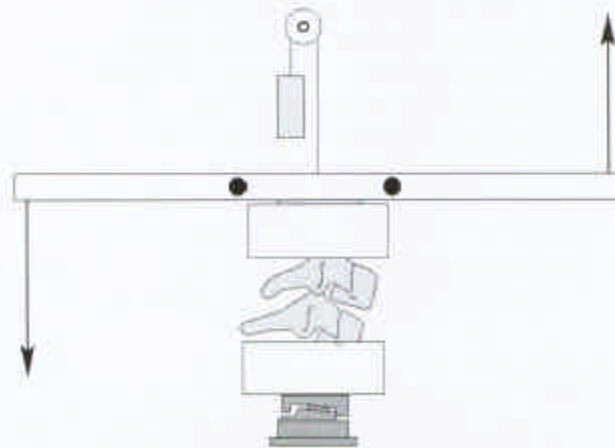


Figure 2. A schematic of the apparatus used to apply pure flexion and extension moments. Optical markers on the couple arm were tracked to calculate angular displacements. A 6-axis load cell was used to measure the applied moment. The O-C2 spinal units were inverted and were attached to the load cell via halo fixation. A counterbalance mass was used to minimize the loads imposed by the load-arm and casting cup.

Data Analysis

After experimentation, force-displacement responses from the 300 N stiffness test in tension and the approximately ± 3.5 N-m flexibility test in bending were regressed. In order to find the best functional relationship between the applied load and the resulting displacement, three different functions were used for data regression.

$$F = A(e^{Bx} - 1) \quad (1)$$

$$F = Ax^2 + Bx + C \quad (2)$$

$$F = Ax + B \quad (3)$$

In these general forms, F represents the applied load, pure tension or pure moment, and x represents the recorded primary displacements axial deflection or angular deflection, respectively.

Because the recorded load data were not identical for all specimens, individual segment stiffness tests were regressed for each function using a nonlinear least squares approach. An average response was then calculated for each motion segment and loading mode based on each function. The average response was the average of the computed values from the individual fits calculated at incremental loads to the end of the regression range, defined as the lowest common load for all specimens. For tension, 1 Newton increments were used to the maximum common load of 300 N. For bending, 0.1 N-m increments were used to the maximum common moment, which was 2 N-m for O-C2 and 3 N-m for the lower cervical spine (LCS) motion segments. A second fit, y_{fit} , was performed on the average response, y_{exp} , and the regressed coefficients and coefficients of determination, R^2 , (Kvalseth, 1985) were determined.

$$R^2 = 1 - \frac{\sum (y_{exp} - y_{fit})^2}{\sum (y_{exp} - \bar{y}_{exp})^2} \quad (4)$$

After the regression of the average responses, two types of extrapolation techniques were used: (a) the continuation of the regressed function; and (b) the linear extrapolation of exponential regression based on the instantaneous slope at the maximum load in the regressed region. These two techniques resulted in four extrapolation functions. The continuations of the regressed functions included the extrapolation of the exponential regression function, the extrapolation of the quadratic regression function, and the extrapolation of the linear regression function. The fourth extrapolation function was the linear extrapolation of the exponential regression function. For tension, the slope for the linear extrapolation was the instantaneous slope at 300 N. For bending, the slope was the instantaneous slope at the end of the regression range (2 N-m for O-C2 and 3 N-m for LCS). To assess the performance of each extrapolation function, each function by motion segment and load condition was extrapolated beyond average failure.

The ability of the extrapolation functions to predict failure was evaluated using two methods. First, an average and standard deviation of the failure event, load and displacement, were determined. Each combination of average and standard deviation was used to create a reasonable failure target zone, an ellipse, for the extrapolations. The extrapolated curves were plotted with their respective failure target ellipses. Target average load and displacement zones provided a visual indicator of the performance of the extrapolation of the average response. Second for each specimen by motion segment and load condition, the force error was calculated at each recorded displacement throughout the entire load-displacement response to the actual failure event. The force error was

defined as the difference between the regressed and extrapolated force value, F_{re} , and the recorded experimental force value, F_{exp} . The force error RMS value (5) was then calculated. This measure of error was calculated throughout the load range to failure. Multiple comparisons testing (Tukey) of the maximum force error RMS values was used to determine if there was any difference between the various extrapolation functions for a given motion segment level and mode of loading. All statistical analysis was done at a significance level of 0.05.

$$F_{error,RMS} = \sqrt{\frac{\sum_{i=1}^n (F_{i,exp} - F_{i,re})^2}{n}} \quad (5)$$

RESULTS

Tension

Every regressed function fit the average tension responses well (average $R^2 = 0.9954$) for all motion segments (Table 1). In general, nonlinear functions fit better than the linear expression, and O-C2 responses were most nonlinear. The failure target zones were determined (Table 2, Figure 3b). The extent of the extrapolation was large as the nondestructive tests represent less than 20% of load to failure (Figure 3b).

Table 1. TENSION REGRESSION RESULTS.

EXPONENTIAL: $F_z = a(e^{bz} - 1)$				
	a (N)	b (1/mm)	SLOPE 300N	AVERAGE R^2
O-C2	229	0.506	268	0.9985
C4-C5	1008	0.251	329	0.9951
C6-C7	859	0.223	258	0.9971
QUADRATIC: $F_z = A z^2 + B z + C$				
	A (N/mm ²)	B (N/mm)	C (N)	AVERAGE R^2
O-C2	43.8	108.9	-0.9	0.9988
C4-C5	103.8	173.2	16.8	0.9955
C6-C7	25.9	185.5	2.8	0.9980
LINEAR: $F_z = a_L z + b_L$				
	a_L (N/mm)	b_L (N)	AVERAGE R^2	
O-C2	180	-18.1	0.9850	
C4-C5	283	-1.4	0.9951	
C6-C7	219	-3.5	0.9955	

Table 2. AVERAGE TENSILE SUB-CATASTROPHIC FAILURE.

	O-C2	C4-C5	C6-C7
LOAD (N)	1883 ± 321	1822 ± 155	1626 ± 154
DISPLACEMENT (mm)	7.05 ± 1.64	7.16 ± 1.18	7.79 ± 0.91

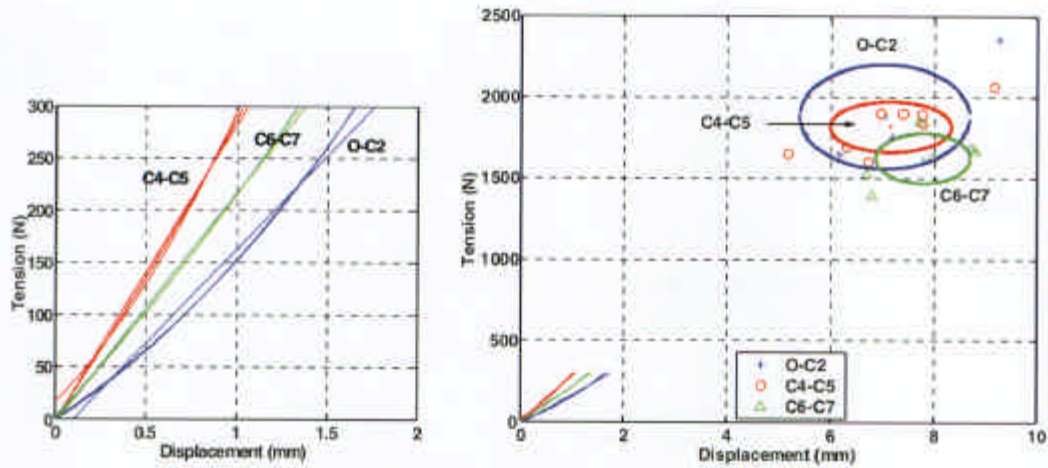


Figure 3. (a) At left, all three regressed functions for the average responses of the motion segments tests. The lower cervical spine is stiffer than upper cervical spine over the loading range of 300 N. (b) At right, failure load and displacement values and target zones for sub-catastrophic failures. O-C2 injuries were varied, including ligamentous disruptions and fractures, causing a larger range of failure loads and displacements.

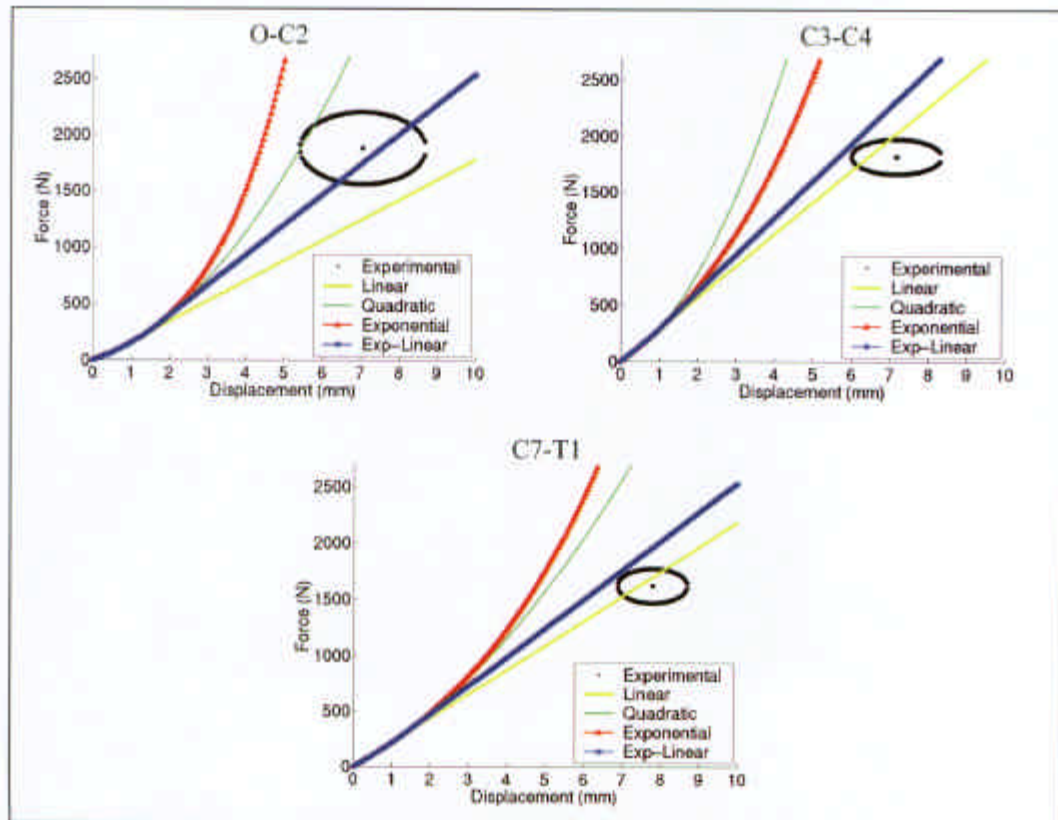


Figure 4. Extrapolation through failure target zones for tension. Nonlinear extrapolations do not model high-load behavior to failure. Linear extrapolations suggest more acceptable behavior paths to failure.

For O-C2, the exponential fit with linear extrapolation best predicted failure (Figure 4) and had the lowest calculated force error RMS values. For C4-C5 and C6-C7, the linear fit best predicted average failure, but it had the highest error RMS values through the regressed region. The linear extrapolation of the exponential fit was the second best predictor of failure. It was not significantly different than the linear fit at failure and provided a better fit to the low-load data.

Bending

Extension (negative moment) and flexion (positive moment) low-load responses were plotted (Figure 5). Exponential functions (average $R^2=0.9986$) had nominally better fits than the quadratic functions (average $R^2=0.9807$) through the low-load region (Table 3), and both were significantly better than the linear function owing to the nonlinearity within the low-load responses.

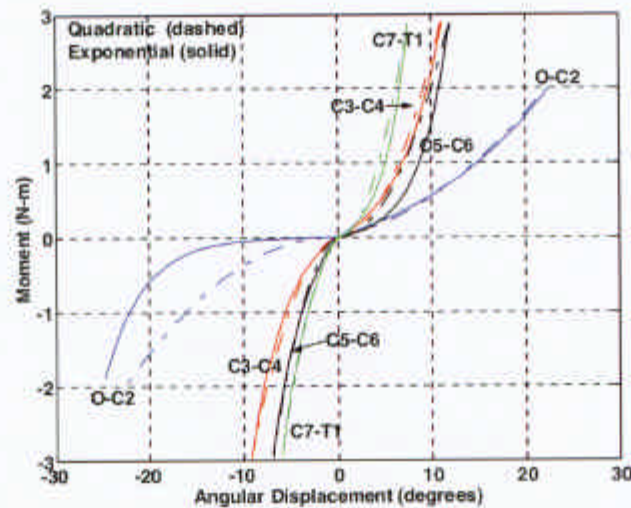


Figure 5. Low-load bending regressions for flexion and extension of the tested motion segments. Flexion is represented with positive values, while extension has negative values. Unlike the tensile responses, the bending data showed a high degree of nonlinearity within this low-load region.

Table 3. BENDING REGRESSION RESULTS.

EXPONENTIAL: $M = 1/B (e^{u/A} - 1)$								
	FLEXION				EXTENSION			
	A (deg)	B (1/N-m)	Slope 2 or 3N-m	R^2	A (deg)	B (1/N-m)	Slope 2 or 3N-m	R^2
O-C2	15.61	1.61	0.17	0.9978	-4.11	-218	0.49	0.9997
C3-C4	4.71	3.41	0.70	0.9974	-3.96	-3.09	0.84	0.9981
C5-C6	3.25	13.68	0.95	0.9995	-4.20	-1.48	0.88	0.9984
C7-T1	2.52	6.67	1.25	0.9987	-3.79	-1.32	0.99	0.9994
QUADRATIC: $M = \theta^2/A + \theta/B$								
	FLEXION			EXTENSION				
	A (deg ²)	B (deg)	R^2	A (deg ²)	B (deg)	R^2		
O-C2	333.33	41.15	0.9920	-243.90	-243.90	0.9433		
C3-C4	42.37	-476.16	0.9909	-32.05	30.03	0.9816		
C5-C6	48.78	-136.99	0.9690	-18.69	20.66	0.9977		
C7-T1	19.19	-125.00	0.9840	-17.51	6.98	0.9874		

The failure target zones were determined (Table 4) and showed the extent of the extrapolation (Figure 6). The low-load range was less than 10% of failure moment for O-C2 and less than 25% of failure moment for lower motion segments.

Table 4. AVERAGE FLEXION AND EXTENSION FAILURES.

	FLEXION		EXTENSION	
	MOMENT (N-m)	ANGLE (deg)	MOMENT (N-m)	ANGLE (deg)
O-C2	23.66 ± 3.42	56.23 ± 2.80	-39.70 ± 12.17	-47.84 ± 11.72
C3-C4	12.02 ± 2.35	16.33 ± 1.77	-18.23 ± 6.00	-23.00 ± 9.32
C5-C6	15.68 ± 2.54	22.97 ± 5.62	-16.40 ± 5.31	-16.58 ± 3.32
C7-T1	23.93 ± 6.91	16.38 ± 6.00	-26.46 ± 8.68	-20.91 ± 7.07

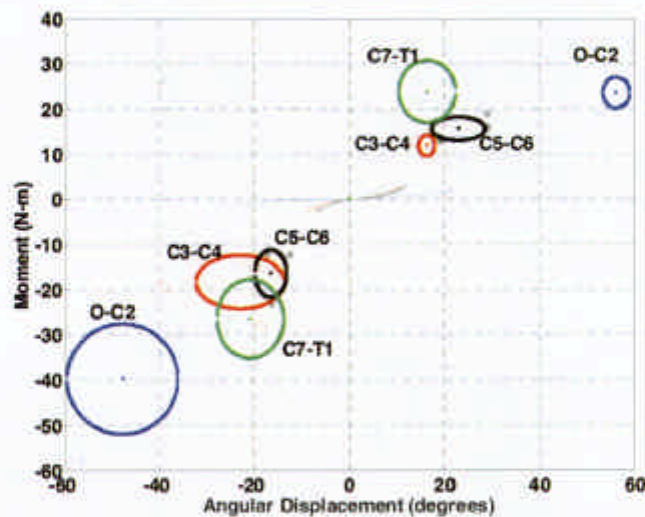


Figure 6. Failure load and displacement values and zones for extension and flexion. Low-load bending responses cover no more than 10% (O-C2) to 25% (C3-C4) of the load response to failure, but exceed 40% (extension) and 30% (flexion) of the angular displacement response.

There was no single best extrapolation function to predict the failure ellipse (Figure 7). However, nonlinear functions were better than the linear functions. In most cases, the stiffness decreased from exponential to quadratic to linear extrapolations. As a result, the rapid stiffening behavior to failure of O-C2 in extension was predicted best by the exponential extrapolation ($p < 0.05$). No other statistically significant differences were observed.

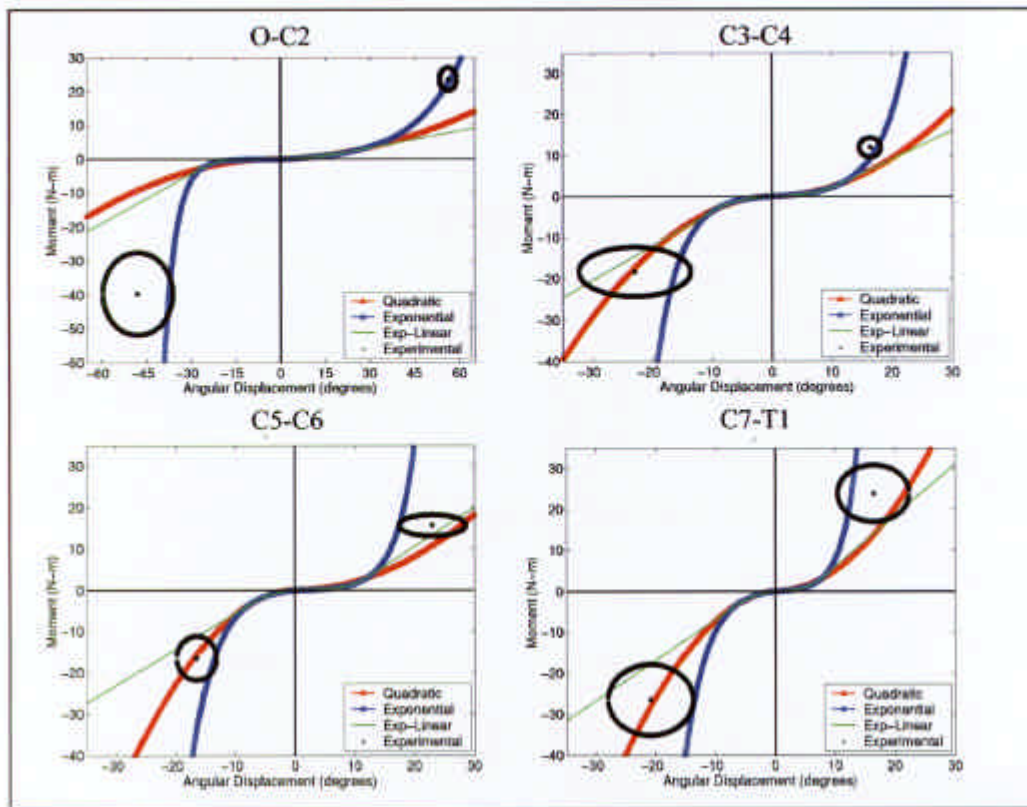


Figure 7. Extrapolation through bending failure target zones. Exponential extrapolation stiffens quickly in the high-load region.

DISCUSSION

Frequently, published biomechanical data do not fully characterize the low-load, high-load, and failure properties of structures in a given mode of loading. And yet, such data are required for numerical study of biomechanical systems. Investigators are therefore compelled to extrapolate low-load data up to failure, despite the probability of significant error. In this study we examined two different data sets to determine which extrapolation functions best predict high-load responses from low-load data. Unfortunately, no single function performed best with all data sets. However by studying the low-load data, better choices of functions became apparent.

While nonlinear regression functions fit the low-load data best, the degree of nonlinearity in the low-load data helps to differentiate between extrapolation functions. Nonlinear extrapolations better predicted failure for the more nonlinear low-load data, but linear extrapolations better predicted failure for the less nonlinear low-load data. Low-load data that are more highly nonlinear, such as the bending data, are better described by more nonlinear extrapolation, like the exponential extrapolation. By contrast, if the data are only modestly nonlinear, such as the tension data, in the low-load region, linear functions and less nonlinear functions perform better, like the linear extrapolation and the linear extrapolation of the exponential regression function. Specifically, the linear extrapolation of the exponential regression function in tension provided good overall, low and high, load-displacement behavior. In regard to overall performance, the linear extrapolation of the exponential regression function appears to be the best selection if data are limited.

There were several limitations of this study. Only two data sets were available for examination with similar experimental conditions for both low-load and failure testing. However, low-load and failure testing occurred at different loading rates. Differences also existed between the two studies because two distinct failure criteria were used. The tension study including sub-catastrophic failures, while the bending study only included ultimate failures. The ultimate failure criterion shifts the average failure zone to the right with respect to the sub-catastrophic zone. Thus decreasing the importance of nonlinear stiffening behavior of the extrapolation. For this reason, the extrapolation of the exponential function is an even more appealing choice for predicting high-load behavior for the highly nonlinear bending data.

CONCLUSIONS

While numerous types of regression functions exist, these functions must conform to the shape of the data and be consistent with behavior past regression ranges. Even if higher loads are not applied in the testing protocol, reasonable expectations are required of regression and extrapolation functions for increasing loads. Without extending the experimental loading range, well-reported failures and the degree of nonlinearity in the low-load data can give clues as to the most suitable extrapolation functions. As a result, different modes of loading of the same structure may be best represented by different extrapolation functions. This work found that the linear extrapolation of the average exponential regression function is best for the average tensile response of the cervical spine to failure, and the continuation of the average exponential regression function is preferred for bending of the cervical spine. Absent confident supporting data, the linear extrapolation of the exponential regression function is the best for both fitting low-load data and approximating high-load behavior.

ACKNOWLEDGEMENTS

This study was supported by the National Highway Traffic Safety Administration cooperative agreement DTNH22-94-Y-07133.

REFERENCES

- CAVANAUGH, J. M. and KING, A. I. (1990). Control of transmission of hiv and other bloodborne pathogens in biomechanical cadaveric testing. *Journal of Orthopaedic Research*, 8, 159-166.
- KVALSETH, T. O. (1985). Cautionary note about R^2 . *The American Statistician*, 39, 279-285.
- MATSUSHITA, T., SATO, T. B., HIRABAYASHI, K., FUJIMURA, S., ASAZUMA, T., and TAKATORI, T. (1994). X-Ray study of the human neck motion due to head inertia loading. *Proc. 38rd Stapp Car Crash Conference*, SAE Paper No. 942208, 55-64.
- MCELHANEY, J. H., HOPPER, R. H., NIGHTINGALE, R. W., and MYERS, B. S. (1995). Mechanisms of basilar skull fracture. *Journal of Neurotrauma*, 12, 669-678.
- NIGHTINGALE, R. W., WINKELSTEIN, B. A., KNAUB, K. E., RICHARDSON, W. J., LUCK, J. F., and MYERS, B. S. (2002). Comparative strengths and structural properties of the upper and lower cervical spine in flexion and extension. *Journal of Biomechanics*, 35, 725-732.
- VAN EE, C. A., NIGHTINGALE, R. W., CAMACHO, D. L. A., CHANCEY, V. C., KNAUB, K. E., SUN, E. A., and MYERS, B. S. (2000). Tensile properties of the human muscular and ligamentous cervical spine. *Stapp Car Crash Journal*, 44, 85-102.

DISCUSSION

PAPER: Selection of Extrapolation Function for the Prediction of High-Load Responses from Low-Load Biomechanical Data

PRESENTER: *Barry Myers, Duke University*

QUESTION: *Erik takhounts, NHTSA*

It looks like a bilinear fit will work pretty well too with the data you presented?

A: I agree with you actually and I've been yelling at my student to give me a bilinear fit of the data. Just some sort of piece-wise linear fit is classic. The place I saw it first is in vascular studies because you've got this deflated vessel, you inflate it with some modest pressure and it's fairly linear as you inflate it further and you just extrapolate that line back to zero and then you have a piece-wise linear fit.

Q: How about continuity condition and that's all?

A: Yes. The downside to it is it's very tender to the domain you choose to fit the second you're sloped to and you end up making some sort of ad hoc choice which is one reason not to do it. However, I agree with you and I was bugging him to get me that data before this talk but they were working pretty hard already.

Q: *Guy Nusholtz, Daimler Chrysler*

The general form of how you're fitting that sort of requires that the intermediate values will fall on that curve that you're generating and that's not necessarily going to be the case either for softening or stiffening and then softening. And it would be sort of a risk to try and do something like that unless you had maybe a couple intermediate values to make sure you're coming through to hit your failure criteria?

A: As a general proposition that marries up with Jeff's comments and I agree with you. What I can tell you, I used that as a model for this data to give me a metric that was simple and easily illustrated. In the context of structures like ligament, inter-vertebral discs, the data are very well behaved, it gets stiffer and then fails. So you actually know what you got and if you look at the extrapolation, if you look at the data through that intermediate range it follows the same conclusions.

Q: But then you know the form of the data before you did it. So you can almost choose that form to fit the curve width?

A: Agreed. On the other hand, if I were testing some generic structure and I felt that it was like a ligament I would use those models. On the other hand, if it was like a brain or like a muscle I might have to think twice about it.

Q: But then once again you already know the form. Okay. Thank you.